Nanolignocellulose extracted from environmentally undesired prosopis juliflora

(article starts on next page)

Nanolignocellulose Extracted from Environmentally Undesired *Prosopis juliflora*

Luis Valencia,[†,∥] Vishnu Arumughan,[‡,§,∥] Blanca Jalvo,[†] Hanna J. Maria,[§] Sabu Thomas,[§] and Aji P. Mathew*[†]

[†]Division of Materials and Environmental Chemistry, Stockholm University, Frescativägen 8, 10691 Stockholm, Sweden
[‡]Chemistry and Chemical Engineering, Chalmers University of Technology, Kemigarden 4, SE-41296 Gothenburg, Sweden
[§]International and Inter University Centre for Nanoscience and Nanotechnology (IIUCNN), M.G. University, 686560 Kottayam, Kerala

S *Supporting Information*

ABSTRACT: Rising sustainability demands the search of new low-market-value sources of lignocellulosic biomass as raw material for nanocellulose processing. In this paper, we accordingly propose the isolation of nanocellulose from *Prosopis juliflora*, an abundant but environmentally undesired tree. *P. juliflora* wood was powered, refined by steam explosion and bleaching, and subsequently used to isolate cellulose nanocrystals and nanofibers by means of acid hydrolysis and mechanical fibrillation. The derived nanocrystals had a rod-shaped structure with an average diameter of 20 nm and length of 150 nm, whereas the nanofibers had a diameter of 10 nm and length in micron size. Moreover, we report a simple method to isolate nanolignocellulose by using partially bleached *P. juliflora* as feedstock. The presence of lignin provided antioxidant and antimicrobial activity to nanocellulose, as well as hydrophobicity and increased thermal stability. The study demonstrates the successful use of *P. juliflora* to extract functional nanomaterials, which compensate for its environmental concern and declining market interest.

INTRODUCTION

Wood is considered one of the most successful engineering materials on earth, which has sustained life, environment, and human society for several centuries. The cell wall is rich in cellulose, lignin, and hemicellulose, where cellulose is the load-bearing entity, whereas lignin and hemicellulose act as the polymer matrix. Nanocellulose, isolated through a top-down approach, has generated great interest as a reinforcement and a building block for functional nanomaterials due to its renewability, biocompatibility, high specific surface area, low density, and good mechanical properties.[1,2] There is an ongoing effort to produce nanocellulose more economically and energy efficiently, for which waste biomaterials (agricultural residues,[3] industrial residues,[4] sidestreams,[5] etc.) are being explored.

Prosopis juliflora is a woody, nitrogen-fixing plant that grows to a height of 5−10 m and is native from South and Central America. This plant can grow in semiarid regions and even under harsh environmental conditions but has declining market interest[6−8] due to its invasive nature. *P. juliflora* has invaded India and other regions throughout the world including Saharan and southern Africa, the Middle Eaast, Pakistan, and Hawaii,[9] where it appears to suppress species native to those regions, besides altering ecosystem services such as water supply, hydrological functioning, grazing potential, and soil quality.[10] The chemical composition of *P.*

juliflora has been reported earlier as cellulose 40−45%, hemicellulose 25−30%, lignin 11−28%, and extractives (sugar, resins, volatile oils, fatty acids, tannins, alcohol, and phenols) 3−15%.[11,12] Multiple attempts to introduce a potential application to *P. juliflora* have been previously reported;[13−16] however, there are no reports about the extraction of nanocellulose from *P. juliflora* yet.

In this work, we explore *P. juliflora* as a source of cellulose nanocrystals (CNCs) and nanofibers (CNFs) and also report the isolation of nanolignocellulose (L-CNC and L-CNF) by simply using partially bleached *P. juliflora* as feedstock. Lignin, considered as a side product in the extraction of cellulose, typically needs to be removed for most applications. However, it has been previously proved that the presence of a certain amount of residual lignin in nanocellulose can actually improve the dispersion and compatibility of nanocellulose in hydrophobic polymeric matrices and nonpolar solvents (without affecting intrinsic properties),[2] as well as acting as an effective free radical scavenger that stabilizes the reactions induced by oxygen and its radical species.[17−19] Moreover, the complete removal of lignin from cellulose requires exhaustive bleaching processes, which increases the commercial value of nano-

cellulose, as well as generating a great amount of hazardous waste. Consequently, there is a rising interest in the use of partially bleached pulp as feedstock for lignocellulose, where the properties of lignin can also be utilized.[20−22] We demonstrated that the presence of this lignin layer on nanocellulose (confirmed by scanning transmission electron microscopy (STEM) and X-ray photoelectron spectroscopy (XPS)) tunes the hydrophobicity, thermal stability, and surface charge of nanocellulose, besides enhancing their antioxidant and antimicrobial activities. The significance of this work lies in the potential for low-cost eco-friendly materials in terms of renewability and sustainability by having the possibility of utilizing environmentally undesired *P. juliflora* in daily life applications.

■ EXPERIMENTAL PART

Materials. *P. juliflora* was collected from Gujarat, India. All chemicals, that is, ethanol (anhydrous, histological grade, Fisher Scientific), hydrochloric acid (HCl, 1 M, Fisher Scientific), sulfuric acid (H$_2$SO$_4$, 64 wt %, Fisher Scientific), sodium hydroxide (NaOH, 1 M, Fisher Scientific), sodium hypochlorite (NaClO, 10.6%, reagent grade, Sigma-Aldrich), glacial acetic acid (Sigma-Aldrich), oxalic acid (Sigma-Aldrich), 2,2-diphenyl-1-picrylhydrazyl (DPPH) (Sigma-Aldrich), ascorbic acid (Sigma-Aldrich), polyphenol oxidase (PPO) from mushroom (Sigma-Aldrich), and catechol (Sigma-Aldrich), were used as received.

Cellulose Extraction. *P. juliflora* was cut and ground into fine powder of 30−100 μm (see the Supporting Information, Figure S1). The *P. juliflora* powder was washed several times with water and then treated three times with 5 wt % NaOH solution in an autoclave kept at 110 °C and 137 Pa for 30 min in order to remove hemicellulose, lignin, and other impurities by saponification and cleavage of lignin−carbohydrate linkages.[23] Then, the fibers were partially bleached using a mixture of NaOH and acetic acid (27 and 78.8 g, respectively) and sodium chlorite solution. This process was repeated six times. The fibers were thereafter thoroughly washed and subjected to oxalic acid treatment coupled with steam explosion, where the lignocellulosic material was loaded directly into the steam gun and treated with high-pressure steam at a temperature of 100−150 °C followed by sudden release of pressure. This method has been reported to be very efficient to open up the lignocellulosic structure of the fibers, reducing significantly the amount of chemicals needed for the extraction process.[24−26] This product is termed "partially bleached" feedstock and converted to nanocellulose as described below by a mechanical and acid hydrolysis process to obtain lignin-containing cellulose nanofiber and nanocrystals, respectively. The product was also bleached further prior to mechanical treatment and acid hydrolysis process to obtain cellulose nanofiber and nanocrystals with no or low amount of lignin. A schematic for the isolation procedure is given in Figure 1.

Isolation of Nanocellulose. Cellulose nanofibers (CNFs) were prepared by means of mechanical fibrillation of *P. juliflora* fibers using an ultrafine friction grinder (Masuko Super-masscolloider, model MKZA 10-15J Corp., Japan) at 1500 rpm. The suspension (2 wt %) with a batch size of 2 L was passed through the grinder seven times to obtain a thick gel of nanofibers, and the processing time was 40 min per batch. Cellulose nanocrystal (CNC) suspension was prepared by sulfuric acid hydrolysis with 64 wt % sulfuric acid at 45 °C under vigorous stirring, following the process reported by
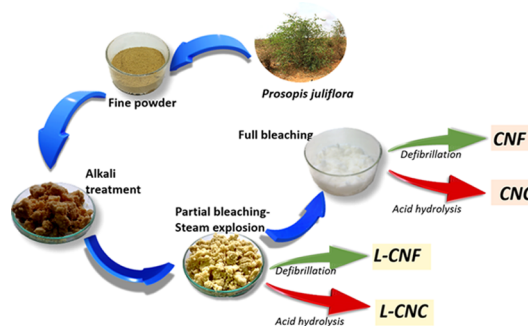

Figure 1. Schematic illustration of the extraction process of nanocellulose from *P. juliflora*.

Bondeson et al.[27] The reaction was quenched by adding an excess of distilled water after 45 min and allowed to cool down to room temperature. The suspension was repeatedly centrifuged at 4000 rpm for 20 min to concentrate the cellulose nanocrystals and to remove the excess of aqueous acid. The resultant nanocrystals were rinsed and dialyzed against deionized water for 5 days until constant neutral pH. The suspension was sonicated using a Qsonica Q500, 500 W Sonicator at 75% output for 2 min.

Characterization of Nanocellulose. The size distribution of nanocellulose was estimated using a scanning transmission electron microscope (STEM) Jeol JEM 2100F with accelerating voltage of 80 kV. For analysis, a droplet of diluted suspension of the sample was deposited on a carbon microgrid prior to examination and allowed to dry. Topographical surface images were captured using an atomic force microscope (AFM, Veeco Multimode V) operating in the tapping mode. The surface charge of the nanocellulose dispersions was studied by ζ-potential measurements using a Zetasizer Nano ZS (Malvern Instruments Ltd., U.K.). The pH of the suspensions was examined before and after measurements; HCl and NaOH were used to adjust the pH to the required values. Moreover, the charge density of CNC was determined by conductometric titration. First, 0.2 g of CNCs was suspended in 20 mL of water. The pH of the solution was adjusted to 2.5 by adding HCl (0.1 M). Then, the suspension was titrated with 0.01 M NaOH. The chemical composition of nanocellulose was analyzed using X-ray photoelectron spectroscopy (Kα XPS, Thermo Scientific, electron spectrometer) with a monochromated Al Kα X-ray source run at 100 W. Survey scans were taken with a 1.0 eV step and 80 eV analyzer pass energy, and the high-resolution regional spectra were recorded with a 0.1 eV step and 20 eV pass energy. The thermal behavior of the nanocellulose samples was assessed by thermogravimetric analyses (TGA) using a TA Instruments Discovery thermal analyzer for measuring the mass transformation as a function of temperature in an interval of 30−600 °C at a heating rate of 5 °C/min. The samples were exposed to nitrogen gas at a flow rate of 20 mL/min. The crystallinity of samples was studied using powder X-ray diffraction (PXRD). The analyses were carried out using a PANalytical X'Pert PRO X-ray system with the settings viz. current 40 mA, tension of 45 kV, at a temperature of 25 °C with step size (2θ) of 0.05. The diffracted intensity of Cu Kα radiation wavelength of 0.1542 was recorded between 10 and 80°. The crystallinity index of nanocellulose was calculated by deconvolution of the XRD spectra, fitting the signal into several Gaussian distributions, and estimating the integral area corresponding to the
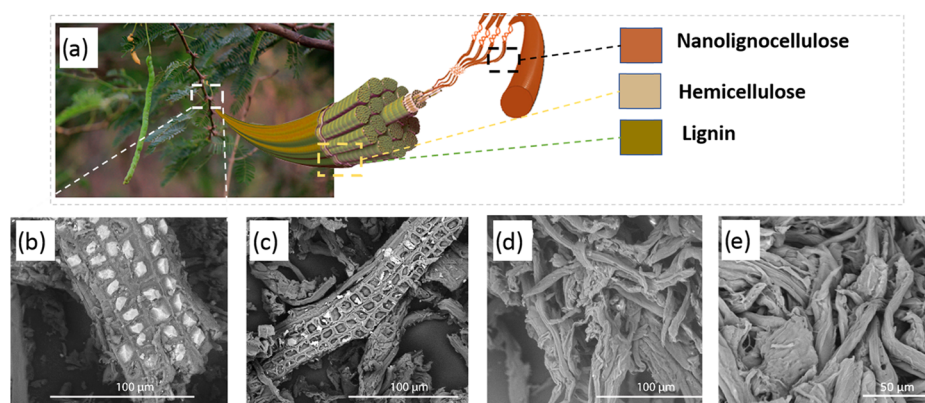
Figure 2. Schematic illustration of the hierarchical structure of *P. juliflora* wood and the corresponding images of the derived products upon each pretreatment stage. (a) Schematic diagram of the three-dimensional microstructure of *P. juliflora*; (b) SEM image of the wood cell wall and SEM images of the derived purified cellulose fibers (c) after alkaline treatment, (d) after steam explosion/partial bleaching, and (e) after full bleaching.

characteristic diffraction peaks of cellulose I polymorph at 18.12° (1 1 0), 22.67° (2 0 0), and 34.5° (0 4 0). The contact angle of the different nanocellulose was evaluated by dropping 1 mL of deionized water by a micro-injector over a nanocellulose film, prepared by solvent evaporation over a glass slide at 60 °C, to be then measured using a digital contact angle instrument with a CCD camera. The contact angle was measured on either side of the drop, and therefore the values were averaged. All measurements were taken within the open air at a relative humidity of 40 ± 5% relative humidity and at a room temperature of 23 °C.

Determination of Antioxidant Activity. The antioxidant activity of the nanocellulose suspensions was determined by the 2,2-diphenyl-1-picrylhydrazyl (DPPH) antioxidant assay and the polyphenol oxidase (PPO) activity quantification.

DPPH Antioxidant Assay. The test consisted of adding certain amounts of the CNF, CNC, L-CNF, and L-CNC (0.49 wt % in all cases) aqueous suspensions into 50 μM DPPH solution in methanol. In addition, ascorbic acid solution (1 mM) was prepared in methanol as a reference standard antioxidant. The reaction mixtures were kept at 30 °C in darkness for 30 min, and then the absorbance was measured at 517 nm over time by using an ultraviolet−visible (UV−vis) spectrophotometer. The experiments were repeated three times, and all measurements were done under dim light.

PPO Activity Determination. Commercial PPO from mushroom was prepared in 0.1 M sodium phosphate buffer at a final concentration of 0.5 wt %. First, 1 mL of the PPO extract was added to a 3 mL catechol solution (80 mM in 0.1 M sodium phosphate buffer), used as a substrate of the enzymatic reaction as described previously.[28] Ascorbic acid was dissolved in aqueous ethanol at a final concentration of the antioxidant of 0.49 wt %. All the samples were kept at pH 6.5 and 25 °C in darkness. The absorbance at 410 nm was recorded at zero time. After 60 s, the increase in absorbance was measured, 100 μL of the 0.49 wt % CNF, CNC, L-CNF, L-CNC, and ascorbic acid solutions were added in the corresponding enzymatic reaction, and the absorbance was recorded immediately at various intervals until the end of the experimental period (600 s). The absorbance change was used to express the PPO activity percentage. The experiments were repeated three times, and all measurements were done under dim light.

Determination of the Antibacterial Activity. The antibacterial susceptibility of nanocellulose suspensions against

Escherichia coli CECT 516 and *Staphylococcus aureus* CECT 240 was evaluated by the disc diffusion method.[29] Briefly, a 100 μL sample of freshly grown bacterial suspension (with a concentration of ~108 CFU/mL) was spread on the nutrient agar plates. Sterile paper disks of uniform size (32 mm) were impregnated with the CNF, CNC, L-CNF, and L-CNC samples and then placed on the nutrient agar plates. After 24 h of incubating the plates at 37 °C, the resulting growth of bacteria was detected and the zone of inhibition (ZOI) was measured.

■ RESULTS AND DISCUSSION

For the extraction of nanocellulose, one must first disintegrate the stem wood into individual cellulose fibrils, which are embedded in a matrix composed of lignin, hemicellulose, and other noncellulosic materials. The extraction is done through the top-down approach (see Figure 2a) submitting the bulk wood into different pretreatment methods like alkali treatment followed by bleaching and steam explosion in the presence of oxalic acid (see Figure 1). The alkali treatment causes the degradation of ester and glycosidic side chain, resulting mainly in structural alteration of lignin, cellulose swelling, and partial decrystallization of cellulose and solvation of hemicellulose. Bleaching, on the other hand, removes the remaining lignin, and steam explosion breaks the lignocellulosic structure through an explosive decompression and rapid depressurization, through which the fibril structure is destroyed. The influence of each pretreatment stage over the lignocellulosic structure of *P. juliflora* was elucidated using scanning electron microscopy (SEM) (Figure 2b−d), where the raw wood particles (Figure 2b) showed evidence of closely packed wax and other noncellulosic components over the surface, which were removed upon alkali treatment (Figure 2c), and subsequently yielded cellulose fibers with a smooth surface after partial bleaching/steam explosion (Figure 2d) as well as complete bleaching (Figure 2e), which goes in agreement with previous reports.[30]

Fourier transform infrared (FTIR) spectroscopy (Figure S1a) was used to follow the chemical changes during each pretreatment stage, where the decreases in the characteristic peaks corresponding to lignin, centered at 1506 cm^{-1} attributed to C═C stretching of aromatic rings of lignin,[31] and hemicellulose, in the range of 1730 cm^{-1} corresponding to the C═O stretching of hemicelluloses,[32] are visible. The increment in degradation temperature, revealed by thermog-
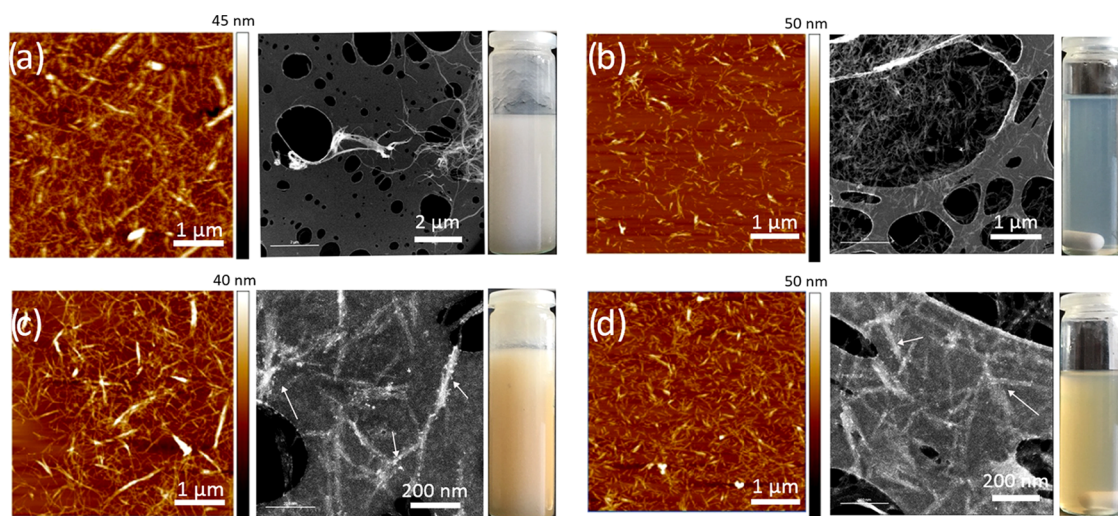
Figure 3. STEM and AFM micrographs of the derived nanocellulose corresponding to (a) CNF, (b) CNC, (c) L-CNF, and (d) L-CNC.

Table 1. Main Characteristics of the Isolated Nanocellulose from *P. juliflora*

sample	diameter (nm)[a]	length (nm)[a]	contact angle (deg)	crystallinity degree (%)[b]	surf. charge (μmol/g)[c]
CNF	10 ± 10	>1 μm	38.8 ± 2.0	70.8 ± 3.5	N.C.[d]
CNC	20 ± 5	150 ± 30	24.7 ± 3.5	76.3 ± 5.6	184.7
L-CNF	40 ± 10	>1 μm	63.0 ± 3.0	58.9 ± 4.5	N.C.[d]
L-CNC	30 ± 5	150 ± 30	67.1 ± 1.9	64.8 ± 2.0	109.2

[a]Estimated by STEM. [b]Calculated using powder X-ray diffraction. [c]Determined by conductometric titration. [d]N.C. = not calculated.
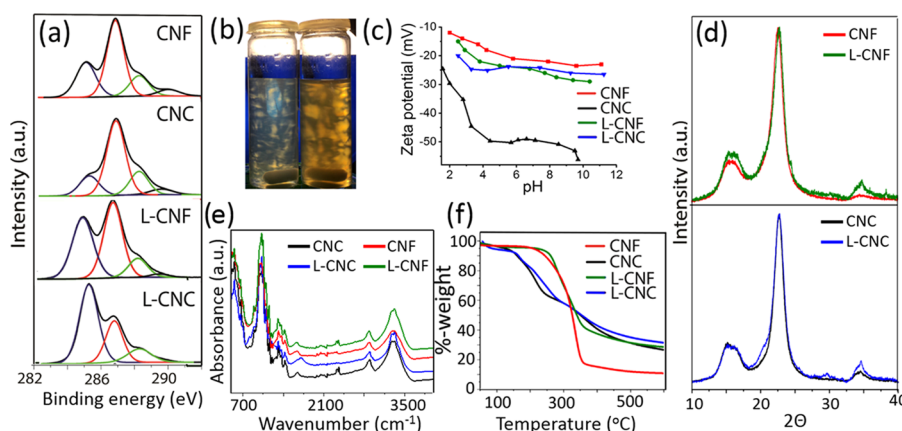

Figure 4. Characterization of nanocellulose obtained from *P. juliflora*. (a) Peak-fitted high-resolution C 1s XPS spectra; (b) birefringence of CNC and L-CNC; (c) ζ-potential values as a function of pH; (d) XRD spectra, (e) FTIR spectra, and (f) TGA thermogram of nanocellulose from *P. Juliflora*.

ravimetric analysis (TGA) (Figure S1b), suggests the removal of hemicellulose from the raw wood powder.[33] The increase in crystallinity after each pretreatment stage, revealed by X-ray diffraction (Figure S1c), also corroborated the results from FTIR and TGA. The significant increase in crystallinity during cellulose fiber isolation confirms the efficient removal of noncellulosic polysaccharides and dissolution of amorphous zones of the fibers. The isolated fibers display the characteristic diffraction peaks at 18.12° (1 1 0), 22.67° (2 0 0), and 34.5° (0 4 0) that correspond to cellulose I polymorph. The % crystallinity of bleached *P. juliflora* fiber was found to be 60%, which is lower than softwood fibers (67%) and plant fibers such as jute (71%)[34] and hemp (88%).[34]

Extraction of Nanocellulose from *P. juliflora*. In this work, we report the successful extraction of CNC and CNF from fully bleached *P. juliflora*, as well as lignin-containing nanocrystals and nanofibers (here denoted L-CNC and L-CNF, respectively), from partially bleached *P. juliflora* feedstock. The size and topography of *P. juliflora* nanocellulose were studied by STEM and AFM (Figure 3), and results are presented in Table 1.

Both CNF and L-CNF (Figure 3a,c) exhibited a fibrillar network structure with average diameters of 10 and 40 ± 10 nm, respectively, and length in the micron scale. The CNCs (Figure 3b,d), on the other hand, exhibited a typical rodlike structure with an average cross-sectional dimension of 20 ± 5 nm and length of 150 ± 30 nm, whose values are similar to the ones found in cotton and sugar beet pulp[35] Moreover, in the case of L-CNC, a significant increase in cross-sectional diameter was observed, displaying an average diameter of 30

± 5 nm. Both CNC and L-CNC suspensions were isotropic, but when the suspensions were shaken, they became intensely birefringent (see Figure 4b (left)), confirming that the ability to form a chiral nematic liquid crystalline phase (in equilibrium with the isotropic phase) was unaffected by the presence of lignin. In the case of L-CNF as well as L-CNC, the increase in diameter is attributed to the presence of a lignin layer on the surface (see Figure 3c), while the length remained unchanged (see Table 1). The high-resolution STEM images show that the L-CNF and L-CNC surfaces were decorated with spherical structures (shown in Figure 3 with white arrows), which are probably due to the presence of a lignin layer over the nanoparticles.

The presence of residual lignin in the nanolignocellulose extracted from *Prosopis Juliflora* was also demonstrated by FTIR spectroscopy (see Figure 4e), where a characteristic band at 1700−1720 cm^{-1} was observed, corresponding to unconjugated carbonyl/carboxyl stretching.[36] On the other hand, the phenolic structure of lignin could not be identified in FTIR spectra as the characteristic aromatic groups were overlapped with the abundant hydroxyl groups of cellulose around 3410−3460 cm^{-1}.[36]

X-ray photoelectron spectroscopy (XPS) was used to demonstrate the presence of lignin on the surfaces of L-CNC and L-CNF by analyzing the deconvoluted high-resolution C 1s spectra (see Figure 4a). For lignin determination, the focus was on the aliphatic carbon regions (designated as C1) centered at 285.0 eV as ideally cellulose is devoid of C1 carbon because of its polysaccharide structure. Therefore, the significant increase in the C1 peak intensity for nanocellulose confirms the presence of lignin over the surface of the nanoparticles when partially bleached *P. juliflora* cellulose was used as feedstock.[37,38] The deconvoluted integral areas of each chemical state of carbon in the C 1s spectra, presented in Table 2, give an indication of the amount of lignin

Table 2. XPS C 1s High-Resolution Data for *P. juliflora* Nanocellulose

sample	binding energy (eV)			
	285 (C1)	287 (C2)	288 (C3)	289 (C4)
CNC	10.91%	70.68%	14.52%	3.89%
CNF	19.84%	63.93%	13.11%	3.12%
L-CNC	58.65%	28.39%	11.8%	1.16%
L-CNF	40.34%	41.2%	13.22%	5.24%

coating the surface of nanocellulose. On the other hand, several physical and chemical changes in the structure of lignin could be also expected caused by the strong pretreatment chemicals such as cleavage of intralignin unit linkages such as β-O-4 ether bonds or formation of new carbon−carbon bonds during severe acid treatment, which could dramatically change the physicochemical properties of lignin, such as functional groups (methoxy, aliphatic hydroxyl, and phenolic hydroxyl).[39]

We evaluated the influence of lignin on the final properties of the nanolignocelluloses considering that the complex polyphenolic structure and numerous functional groups of lignin could provide a significant impact over the properties of nanocellulose. First, the influence of lignin over the surface polarity was evaluated by means of static water contact angle measurements (see Table 1), where neat CNC and CNF exhibited a hydrophilic character with contact angles of 24 and 38°, respectively, whose values are characteristic from cellulose.

However, the wettability significantly decreased for L-CNC and L-CNF, which exhibited contact angle values of 67 and 63°, respectively, attributed to the hydrophobic lignin layer that interacts with the surface of cellulose, masking the reactive hydroxyl groups.

The thermal degradation behavior was studied by means of TGA, and results are presented in Figure 4f. The nanocrystals clearly showed a lower thermal stability compared to the nanofibers due to the presence of sulfate groups, which leads to a faster reduction in degrees of polymerization and degradation at lower temperature.[40] In addition, the thermal degradation of CNF with lignin (L-CNF) was slower at temperatures above 350 °C, which is due to the complex phenolic structure of the residual lignin, which partially decomposes at temperatures above 300 °C; for instance, the β-O-4 bond scission and breaking down of the β-aryl-alkyl-ether bond occur at >300 °C. Moreover, at even higher temperatures (around 400 °C), the C−C bond between lignin structural aromatic rings and α-carbon atom decomposes.[41] The char content was significantly higher for both L-CNC and L-CNF compared to pristine nanocellulose as it is known that lignin produces more char and tar than wood.[41]

The crystallinity (CrI) of the nanocellulose was estimated from X-ray diffraction curves (see Table 1 and Figure 4d), and the crystallinities for L-CNC and L-CNF were lower by approx. 11% compared to neat CNC and CNF and attributed to the amorphous nature of lignin.

The surface charge of the nanocellulose was investigated by ζ-potential measurements (see Figure 4c). All the studied nanocellulose materials exhibit negative ζ-potential values, which originated from different types of surface groups and resultant surface chemistry. The negative ζ-potentials of CNF and L-CNF are attributable to the negatively charged carboxyl groups arising from the bleaching steps, as confirmed by the presence of the C4 peak in the C 1s high-resolution XPS spectra (see Figure 4a and Table 2). On the other hand, L-CNF displayed a lower ζ-potential value than pristine CNF, which is possibly explained by the formation of phenolic methoxy and carboxyl groups on lignin during the strong pretreatment stages. This was corroborated also with the higher percentage of C4 in the C 1s XPS spectra, compared to CNF (see Table 2) and is in agreement with the high-resolution O 1s spectra (see Figure S3), at which both CNF and L-CNF were deconvoluted using two Voigt distributions centered on 532 and 532.8 eV, corresponding to the C−OH and COOH groups, respectively. The negative ζ-potentials exhibited by CNC and L-CNC are attributable to the sulfate groups on the nanocrystals, which are introduced during sulfuric acid hydrolysis. However, CNC exhibited a significantly lower ζ-potential than L-CNC, which suggests that the residual lignin could have partially prevented the sulfonation of the cellulosic structure. This assumption is in agreement with the surface charge density values calculated by conductometric titration; L-CNC exhibited a lower surface charge (109.21 μmol/g) compared to neat CNC (184.73 μmol/g), which corresponds to a 40% decrease in the amount of sulfate groups available in the surface of the L-CNCs.

Antioxidant Activity of Nanolignocellulose. The antioxidant activity of lignin is known to arise from the scavenging action of its phenolic structures on oxygen containing free radicals.[42−44] To determine the antioxidant activity of our extracted nanolignocellulose, we utilized two different approaches: using 1,1-diphenyl-2-picrylhydrazyl
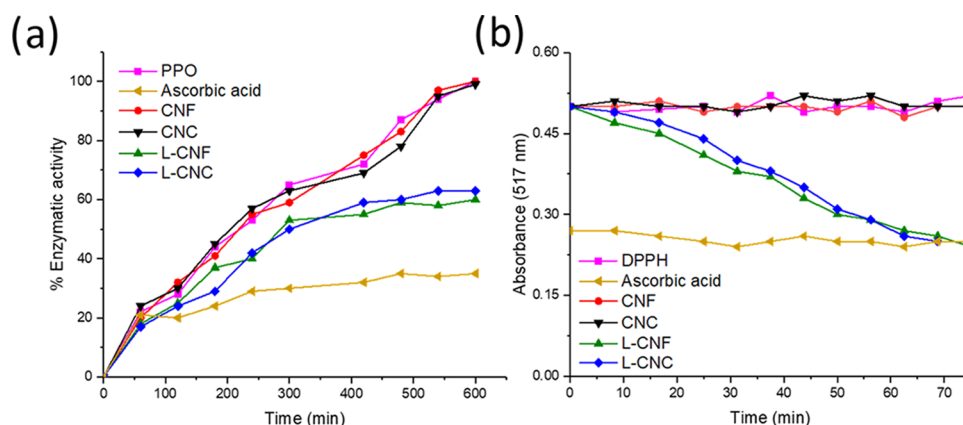
Figure 5. Antioxidant activity of *P. juliflora* nanocellulose: (a) inhibition of PPO activity by *P. juliflora* nanocellulose and ascorbic acid as antibrowning agents and (b) time course of scavenging of DPPH.

(DPPH) as a reactive radical and via studying the polyphenol oxidase (PPO) activity. Figure 5b shows the scavenging activities of free radical DPPH over time for 0.49 wt % CNF, L-CNF, CNC, L-CNC, and ascorbic acid in the methanol/DPPH solution. The radical scavenging reaction of ascorbic acid with DPPH was, essentially, instantaneous. On the other hand, the radical scavenging reaction of L-CNF and L-CNC with DPPH was rather slow and time dependent, reaching similar values as the antioxidant of reference, ascorbic acid, after the end of the incubation period. On increasing the incubation time, the absorbance band at 517 nm decreased, whereas the DPPH scavenging activity increased up to 50% after 75 min of incubation for the nanolignocellulose. CNF and CNC samples did not show any DPPH radical scavenging activity, as expected (Figure 5b).

The results of antioxidant activities were then corroborated by PPO activity determination. PPO is a copper-associated enzyme with two binding sites for phenolic substrates, and it is activated by releasing into the cytosol when plant tissues undergo physical damage such as bruising, cutting, or blending. In the presence of atmospheric oxygen and PPO, phenolic substrates can be oxidized to quinones, which then undergo polymerization to yield dark-brown polymers. Because PPO-catalyzed oxidative reaction in fruits and vegetables can negatively affect the appearance, its presence in fresh products could reduce their shelf life and consumer acceptance and, therefore, their economic value.[45,46] We studied the reduction of PPO activity by CNF, L-CNF, CNC, L-CNC, and ascorbic acid as a well-known antioxidant of reference. Figure 5a shows the values of the PPO enzymatic activity versus reaction time. The PPO activity increased linearly for all samples in the initial 60 s due to the quinone formation as a reaction product of the enzymatic oxidation of catechol by PPO before the addition of the suspensions. After that time, the linear increase stopped for ascorbic acid and the nanolignocelluloses (L-CNF and L-CNC), behaving as partial PPO enzyme inhibitors and partial quinone reducers.

This reduction of the PPO activity by L-CNF and L-CNC resulted in approximately 50% of its activity in both cases, whereas this reduction was about 70% for the ascorbic acid reaction. It was previously reported that ascorbic acid showed different behaviors depending on its concentration.[47] At low concentrations (i.e., 0.5%), ascorbic acid is not able to reduce the whole pool of quinones formed in the reaction and, consequently, does not eliminate the browning effect, but it is

able to behave as a partial PPO inhibitor. The lower effect in PPO inactivation with lower concentrations of L-CNF and L-CNC was also observed during this work (data not shown).

Antibacterial Activity of Nanolignocellulose. The antibacterial response induced by nanolignocellulose against *E. coli* and *S. aureus* was investigated through the agar diffusion method, in which if an antibacterial agent is able to diffuse into agar, the inhibition zone becomes evident as a halo around the impregnated disc. The antibacterial activity was investigated by studying the bacterial growth on the agar plates in the presence of nanolignocellulose. Three replicates per sample were performed, and the average of the inhibition zone measurement is the value given in the results showed in Figure 6, where
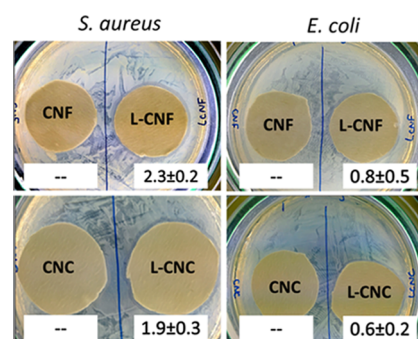

Figure 6. Representative images for the disc diffusion tests of CNF, CNC, L-CNF, and L-CNC suspensions against *S. aureus* and *E. coli*, and the measurement of the average inhibition zones (mm) of the impregnated paper disks.

small inhibition zones for *S. aureus* can be observed (Figure 6), with ZOI values of 2.3 ± 0.2 mm for L-CNF and 1.9 ± 0.3 mm for L-CNC. On the other hand, L-CNF and L-CNC were less effective against *E. coli* with ZOI values of 0.8 ± 0.5 and 0.6 ± 0.2 mm, respectively. For both bacterial strains, there was no bacterial growth directly under the disks impregnated with nanolignocellulose samples. Comparing the antibacterial effects after 24 h, the paper disc impregnated with CNF or CNC without residual lignin did not reduce the growth of any of the bacterial strains studied, as demonstrated by the absence of a halo of growth inhibition around the paper disc.

Dong et al.[48] extracted lignin from the residue of corn, which exhibited antimicrobial activities against Gram-positive bacteria (*Listeria monocytogenes* and *S. aureus*) and yeast (*Candida*

lipolytica), but not Gram-negative bacteria (*E. coli* O157:H7 and *Salmonella enteritidis*). However, in our case, L-CNF and L-CNC exhibited weak antibacterial activities against *E. coli* (Gram-negative bacteria). Yang et al. also reported antibacterial effect of a PLA-based formulation containing lignin nanoparticles (LNPs) and/or a combination of LNP and CNC against different Gram-negative plant pathogenic bacteria, such as *Pseudomonas syringae* pv, tomato, and two different strains of *Xanthomonas* sp. and with higher values than the ones that we obtained in this work.[49] The antibacterial activity of lignin is usually in relation to its phenolic structure and the different functionalities (−OH, −CO, −COOH) acquired throughout the process. Furthermore, it is known that the biocidal activity of lignin is expressed on the bacterial cell membrane, causing severe damages and lysis of bacterial cells with consequent release of cell content.[50]

One plausible reason for the weak antibacterial behaviors of the L-CNF and L-CNC samples could be a fluctuation in the pH toward neutral values due to a microdilution effect during the test method because of the low concentration of lignin available for our experiments. It has been reported that commercial lignin possesses extraordinary antimicrobial effect due to its high pH (10.5, 3 wt %, Sigma) and good solubility and diffusion through the agar medium.[49] Our L-CNF and L-CNC suspensions had pH values of 4.89 and 5.56, respectively, and they could be fixed on the disc paper, preventing its complete diffusion into the agar plate. All bacterial experiments were carried out under bacterial relevant solution and pH = 7 in the agar plates, with a convenient and specific nutritive medium, which allowed the correct growth of the bacteria used in this work. The samples were tested in an unmodified pH after their extraction in order to keep the pristine structure of the nanocrystals for their testing. The acidic pH from the samples, although could be affecting the correct diffusion of the samples into the agar, did not affect the bacterial cultures since an inhibition halo was not observed around the samples without lignin (CNC and CNF) that were used as reference samples.

Nevertheless, our finding indicates that this inherent antimicrobial property of lignin was retained following its transformation into nanofibers or nanocrystals. Furthermore, the antimicrobial activity of nanolignocellulose, combined with good network properties characteristic of nanocellulose to form robust films (see Figure 7), could suggest the potential
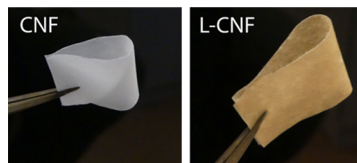

Figure 7. Nanopaper prepared from CNF and L-CNF extracted from *P. juliflora*. The nanopapers were prepared by vacuum filtration of a 2 wt % nanocellulose suspension, followed by drying at room temperature overnight under a constant load of 5 kg.

use of nanolignocellulose in further applications together with a better understanding of its mechanism of action against bacteria and against Gram-negative bacteria in particular.

CONCLUSIONS

Nanocellulose and nanolignocellulose were successfully isolated from *P. juliflora*. The morphological analyses of cellulose

nanocrystals by STEM and AFM confirmed a typical needlelike structure of CNC with a mean cross-sectional size of 20 nm and 150 nm in length, which increased in the presence of lignin particles to 30 nm in diameter. The influence of lignin in the structure of nanolignocellulose was evaluated, whereby an increased hydrophobicity and lower surface charge were confirmed. Furthermore, we demonstrated that the presence of lignin not only enhances the thermal stability but also provides antioxidant and antimicrobial activities to nanocellulose. The results demonstrate the potential for the utilization of environmentally undesired *Prosopis juliflora* in the form of value-added materials as functional CNF and CNC in daily applications such as food packaging.

ASSOCIATED CONTENT

Ⓢ Supporting Information

The Supporting Information is available free of charge on the ACS Publications website at DOI: 10.1021/acsomega.8b02685.

> Experimental procedure of the pretreatment methods of *P. juliflora* cellulose; characterization of cellulose at each pretreatment stage including FTIR spectroscopy; X-ray diffraction and thermogravimetric analysis; XPS survey of nanocellulose extracted from *P. juliflora*, high-resolution O 1s XPS spectra of CNF and L-CNF (PDF)

AUTHOR INFORMATION

Corresponding Author

*E-mail: aji.mathew@mmk.su.se. Phone: +46-721474367.

ORCID Ⓘ

Aji P. Mathew: 0000-0001-8909-3554

Author Contributions

‖L.V. and V.A. contributed equally to this work.

Author Contributions

The manuscript was written through contributions of all authors. All authors have given approval to the final version of the manuscript.

Notes

The authors declare no competing financial interest.

REFERENCES

(1) Mathew, A. P.; Oksman, K.; Sain, M. Mechanical Properties of Biodegradable Composites from Poly Lactic Acid (PLA) and Microcrystalline Cellulose (MCC). *J. Appl. Polym. Sci.* **2005**, *97*, 2014−2025.

(2) Gupta, A.; Simmons, W.; Schueneman, G. T.; Mintz, E. A. Lignin-Coated Cellulose Nanocrystals as Promising Nucleating Agent for Poly (Lactic Acid). *J. Therm. Anal. Calorim.* **2016**, 1243−1251.

(3) García, A.; Gandini, A.; Labidi, J.; Belgacem, N.; Bras, J. Industrial and Crop Wastes: A New Source for Nanocellulose Biorefinery. *Ind. Crops Prod.* **2016**, *93*, 26−38.

(4) Shahabi-Ghahafarrokhi, I.; Khodaiyan, F.; Mousavi, M.; Yousefi, H. Preparation and Characterization of Nanocellulose from Beer

Industrial Residues Using Acid Hydrolysis/Ultrasound. *Fibers Polym.* **2015**, *16*, 529−536.

(5) Dima, S.-O.; Panaitescu, D.-M.; Orban, C.; Ghiurea, M.; Doncea, S.-M.; Fierascu, C. R.; Nistor, L. C.; Alexandrescu, E.; Nicolae, C.-A.; Tricǎ, B.; et al. Bacterial Nanocellulose from Side-Streams of Kombucha Beverages Production: Preparation and Physical-Chemical Properties. *Polymers* **2017**, 374.

(6) Liu, C.; Li, B.; Du, H.; Lv, D.; Zhang, Y.; Yu, G.; Mu, X.; Peng, H. Properties of Nanocellulose Isolated from Corncob Residue Using Sulfuric Acid, Formic Acid, Oxidative and Mechanical Methods. *Carbohydr. Polym.* **2016**, *151*, 716−724.

(7) Jongaroontaprangsee, S.; Chiewchan, N.; Devahastin, S. Production of Nanocellulose from Lime Residues Using Chemical-Free Technology. *Mater. Today: Proc.* **2018**, *5*, 11095−11100.

(8) Ben-Shabat, S.; Kumar, N.; Domb, A. J. PEG-PLA Block Copolymer as Potential Drug Carrier: Preparation and Characterization. *Macromol. Biosci.* **2006**, *6*, 1019−1025.

(9) Van Klinken, R. D.; Graham, J.; Flack, L. K. Population Ecology of Hybrid Mesquite (Prosopis Species) in Western Australia: How Does It Differ from Native Range Invasions and What Are the Implications for Impacts and Management? *Biol. Invasions* **2006**, *8*, 727−741.

(10) Shackleton, R. T.; Le Maitre, D. C.; Pasiecznik, N. M.; Richardson, D. M. Prosopis: A Global Assessment of the Biogeography, Benefits, Impacts and Management of One of the World's Worst Woody Invasive Plant Taxa. *AoB Plants* **2014**, *6*, 1−18.

(11) Prabha, D. S.; Dahms, H. U.; Malliga, P. Pharmacological Potentials of Phenolic Compounds from Prosopis Spp.-a Review. *J. Coastal Life Med.* **2014**, *2*, 918−924.

(12) Gujarat Energy Development Agency. *Role of Prosopis in Wasteland Development: 1st National Workshop: Papers*; Jivrajbhai Patel Agroforestry Centre, 1983.

(13) Kumar, M.; Tamilarasan, R. Removal of Victoria Blue Using Prosopis Juliflora Bark Carbon: Kinetics and Thermodynamic Modeling Studies. *J. Mater. Environ. Sci.* **2014**, *5*, 510−519.

(14) Sennu, P.; Choi, H. J.; Baek, S. G.; Aravindan, V.; Lee, Y. S. Tube-like Carbon for Li-Ion Capacitors Derived from the Environmentally Undesirable Plant: Prosopis Juliflora. *Carbon* **2016**, *98*, 58−66.

(15) Saravanakumar, S. S.; Kumaravel, A.; Nagarajan, T.; Sudhakar, P.; Baskaran, R. Characterization of a Novel Natural Cellulosic Fiber from Prosopis Juliflora Bark. *Carbohydr. Polym.* **2013**, *92*, 1928−1933.

(16) Nascimento, E. S. D.; Lima, H. L. S.; Barroso, M. K. D. A.; Brígida, A. I. S.; Andrade, F. K.; Borges, M. D. F.; Morais, J. P. S.; Muniz, C. R.; Rosa, M. D. F. Mesquite (Prosopis Juliflora (Sw.)) Extract Is an Alternative Nutrient Source for Bacterial Cellulose Production. *J. Biobased Mater. Bioenergy* **2016**, *10*, 63−70.

(17) Dizhbite, T.; Telysheva, G.; Jurkjane, V.; Viesturs, U. Characterization of the Radical Scavenging Activity of Lignins - Natural Antioxidants. *Bioresour. Technol.* **2004**, *95*, 309−317.

(18) Li, Z.; Ge, Y. Antioxidant Activities of Lignin Extracted from Sugarcane Bagasse via Different Chemical Procedures. *Int. J. Biol. Macromol.* **2012**, *51*, 1116−1120.

(19) Lu, F. J.; Chu, L. H.; Gau, R. J. Free Radical-Scavenging Properties of Lignin. *Nutr. Cancer* **1998**, *30*, 31−38.

(20) Morales, L. O.; Iakovlev, M.; Martin-Sampedro, R.; Rahikainen, J. L.; Laine, J.; van Heiningen, A.; Rojas, O. J. Effects of Residual Lignin and Heteropolysaccharides on the Bioconversion of Softwood Lignocellulose Nanofibrils Obtained by SO2−ethanol−water Fractionation. *Bioresour. Technol.* **2014**, *161*, 55−62.

(21) Delgado-Aguilar, M.; González, I.; Tarrés, Q.; Pèlach, M. À.; Alcalà, M.; Mutjé, P. The Key Role of Lignin in the Production of Low-Cost Lignocellulosic Nanofibres for Papermaking Applications. *Ind. Crops Prod.* **2016**, *86*, 295−300.

(22) Nair, S. S.; Kuo, P.-Y.; Chen, H.; Yan, N. Investigating the Effect of Lignin on the Mechanical, Thermal, and Barrier Properties of Cellulose Nanofibril Reinforced Epoxy Composite. *Ind. Crops Prod.* **2017**, *100*, 208−217.

(23) Lee, H. V.; Hamid, S. B. A.; Zain, S. K. Conversion of Lignocellulosic Biomass to Nanocellulose: Structure and Chemical Process. *Sci. World J.* **2014**, *2014*, 1−20.

(24) Espino, E.; Cakir, M.; Domenek, S.; Román-gutiérrez, A. D.; Belgacem, N.; Bras, J. Isolation and Characterization of Cellulose Nanocrystals from Industrial By-Products of Agave Tequilana and Barley. *Ind. Crop. Prod.* **2014**, *62*, 552−559.

(25) Cherian, B. M.; Leão, A. L.; de Souza, S. F.; Thomas, S.; Pothan, L. A.; Kottaisamy, M. Isolation of Nanocellulose from Pineapple Leaf Fibres by Steam Explosion. *Carbohydr. Polym.* **2010**, *81*, 720−725.

(26) Thomas, M. G.; Abraham, E.; Jyotishkumar, P.; Maria, H. J.; Pothen, L. A.; Thomas, S. Nanocelluloses from Jute Fibers and Their Nanocomposites with Natural Rubber: Preparation and Characterization. *Int. J. Biol. Macromol.* **2015**, *81*, 768−777.

(27) Bondeson, D.; Mathew, A.; Oksman, K. Optimization of the Isolation of Nanocrystals from Microcrystalline Cellulose by Acid Hydrolysis. *Cellulose* **2006**, 171−180.

(28) Sharma, O. P.; Bhat, T. K. DPPH Antioxidant Assay Revisited. *Food Chem.* **2009**, *113*, 1202−1205.

(29) Holder, I. A.; Boyce, S. T. Agar Well Diffusion Assay Testing of Bacterial Susceptibility to Various Antimicrobials in Concentrations Non-Toxic for Human Cells in Culture. *Burns* **1994**, *20*, 426−429.

(30) Zaini, L. H.; Jonoobi, M.; Tahir, P.; Karimi, S. Isolation and Characterization of Cellulose Whiskers from Kenaf (*Hibiscus cannabinus* L.) Bast Fibers. *J. Biomater.* **2013**, *2013*, 37−44.

(31) Mtibe, A.; Linganiso, L. Z.; Mathew, A. P.; Oksman, K.; John, M. J.; Anandjiwala, R. D. A Comparative Study on Properties of Micro and Nanopapers Produced from Cellulose and Cellulose Nanofibres. *Carbohydr. Polym.* **2015**, *118*, 1−8.

(32) Fortunati, E.; Luzi, F.; Jiménez, A.; Gopakumar, D. A.; Puglia, D.; Thomas, S.; Kenny, J. M.; Chiralt, A.; Torre, L. Revalorization of Sunflower Stalks as Novel Sources of Cellulose Nanofibrils and Nanocrystals and Their Effect on Wheat Gluten Bionanocomposite Properties. *Carbohydr. Polym.* **2016**, *149*, 357−368.

(33) Chirayil, C. J.; Joy, J.; Mathew, L.; Mozetic, M.; et al. Isolation and Characterization of Cellulose Nanofibrils from Helicteres Isora Plant. *Ind. Crop. Prod.* **2014**, *59*, 27−34.

(34) Mwaikambo, L. Y.; Ansell, M. P. Chemical Modification of Hemp, Sisal, Jute, and Kapok Fibers by Alkalization. *J. Appl. Polym. Sci.* **2002**, *84*, 2222−2234.

(35) Khalil, H. P. S. A.; Davoudpour, Y.; Aprilia, N. A. S.; Mustapha, A. Nanocellulose-Based Polymer Nanocomposite: Isolation, Characterization and Applications. *Nanocellul. Polym. Nanocompos.* **2014**, 273−309.

(36) Boeriu, C. G.; Bravo, D.; Gosselink, R. J. A.; Van Dam, J. E. G. Characterisation of Structure-Dependent Functional Properties of Lignin with Infrared Spectroscopy. *Ind. Crops Prod.* **2004**, *20*, 205−218.

(37) Johansson, L. S.; Campbell, J. M. Reproducible XPS on Biopolymers: Cellulose Studies. *Surf. Interface Anal.* **2004**, *36*, 1018−1022.

(38) Johansson, L.-S.; Campbell, J.; Koljonen, K.; Stenius, P. Evaluation of Surface Lignin on Cellulose Fibers with XPS. *Appl. Surf. Sci.* **1999**, *144−145*, 92−95.

(39) Yang, Q.; Pan, X. Correlation Between Lignin Physicochemical Properties and Inhibition to Enzymatic Hydrolysis of Cellulose. *Biotechnol. Bioeng.* **2016**, *113*, 1213−1224.

(40) Chen, Y.; Tan, T. H.; Lee, H. V.; Hamid, S. B. A. Easy Fabrication of Highly Thermal-Stable Cellulose Nanocrystals Using Cr(NO3)3catalytic Hydrolysis System: A Feasibility Study from Macroto Nano-Dimensions. *Materials* **2017**, *10*, 42.

(41) Aho, A.; Salmi, T.; Murzin, D. Y. Catalytic Pyrolysis of Lignocellulosic Biomass. In *The Role of Catalysis for the Sustainable Production of Bio-fuels and Bio-chemicals*; Elsevier, 2013; pp 137−159.

(42) Saito, S.; Okamoto, Y.; Kawamabata, J. Effects of Alcoholic Solvents on Antiradical Abilities of Protocatechuic Acid and Its Alkyl Esters. *Biosci. Biotechnol. Biochem.* **2004**, *68*, 1221−1227.

(43) Saito, S.; Kawabata, J. Effects of Electron-Withdrawing Substituents on DPPH Radical Scavenging Reactions of Proto-catechuic Acid and Its Analogues in Alcoholic Solvents. *Tetrahedron* **2005**, *61*, 8101−8108.

(44) Ozcelik, B.; Lee, J. H.; Min, D. B. Effects of Light, Oxygen, and PH on the Absorbance of 2,2-Diphenyl-1-picrylhydrazyl. *J. Food Sci.* **2006**, *68*, 487−490.

(45) Nicolas, J. J.; Richard-Forget, F. C.; Goupy, P. M.; Amiot, M.; Aubert, S. Y. Enzymatic Browning Reactions in Apple and Apple Products. *Crit. Rev. Food Sci. Nutr.* **1994**, *34*, 109−157.

(46) Núñez-Delicado, E.; Serrano-Megías, M.; Pérez-López, A. J.; López-Nicolás, J. M. Polyphenol Oxidase from Dominga Table Grape. *J. Agric. Food Chem.* **2005**, *53*, 6087−6093.

(47) Ali, H. M.; El-gizawy, A. M.; El-bassiouny, R. E. I.; Saleh, M. A. Browning Inhibition Mechanisms by Cysteine, Ascorbic Acid and Citric Acid, and Identifying PPO-Catechol-Cysteine Reaction Products. *J. Food Sci. Technol.* **2015**, *52*, 3651−3659.

(48) Dong, X.; Dong, M.; Lu, Y.; Turley, A.; Jin, T.; Wu, C. Antimicrobial and Antioxidant Activities of Lignin from Residue of Corn Stover to Ethanol Production. *Ind. Crops Prod.* **2011**, *34*, 1629−1634.

(49) Yang, W.; Fortunati, E.; Dominici, F.; Giovanale, G.; Mazzaglia, A.; Balestra, G. M.; Kenny, J. M.; Puglia, D. Effect of Cellulose and Lignin on Disintegration, Antimicrobial and Antioxidant Properties of PLA Active Films. *Int. J. Biol. Macromol.* **2016**, *89*, 360−368.

(50) Thomas, S.; Visakh, P. M.; Mathew, A. P. *Advances in Natural Polymers*; Springer, 2013; Vol. *18*.